

Crustal thickening and extension induced by the Great Sumatra–Andaman earthquake of 26 December 2004: revealed by the seismic moment tensor element M_{rr}

J.-Y. Lin · C.-L. Lo · W.-N. Wu · J.-C. Sibuet ·
S.-K. Hsu · Y.-Y. Wen

Received: 4 April 2014 / Accepted: 10 October 2014
© Springer Science+Business Media Dordrecht 2014

Abstract In a complex geological environment, it is generally difficult to assimilate a complete understanding of the main stress regime without being distracted by various fault configurations. In this study, we examine the changes in radial seismic moment (M_{rr}) of earthquakes that occurred in the Sumatra area. This approach allows for simplification of the various focal mechanism solutions by compressive and extensional slip vectors. The results show that the epicenter of the 2004 mainshock is located near the area where the accumulated M_{rr} was highest during the inter-seismic period. Simultaneously, a pattern of negative accumulated M_{rr} observed at depths between 40 and 100 km suggests a down-dip extension mechanism caused by the slab pull effect, which could be strengthened by the locking procedure in shallow portions of the slab. Moreover, the right-lateral strike-slip Sumatra Fault and the left-lateral oceanic fracture zones exhibited positive and negative accumulated M_{rr} prior to and immediately after the 2004 mainshock. This transform of M_{rr} indicates stress release associated with the unlocking of the asperities during the earthquake. Therefore, the distinctly different M_{rr} patterns for the inter- and post-seismic period suggest

that the occurrence of a substantial earthquake could change the intraplate stress state.

Keywords Seismic moment tensor · Subduction zone · 2004 Sumatra–Andaman earthquake · Focal mechanism · Intraplate stress

Introduction

The Andaman–Nicobar region in the Indian Ocean, one of the most seismically active regions in the world, has suffered several destructive earthquakes in the past (Bilham et al. 2005; Verma et al. 1978; Zhou et al. 2002). The occurrence of the Mw 9.3 Sumatra–Andaman earthquake of 26 December 2004 provided valuable material and promoted studies of the rupture process, co- and post-seismic deformation, and rheology in this region (Ammon et al. 2005; Pollitz et al. 2006; Reddy et al. 2010). However, the seismogenic characteristics of such great earthquakes for the inter-seismic period remain undefined because of the complexity of the geological environment and the scarcity of available data.

Earthquake source geometry and magnitude can be described mathematically in terms of the seismic moment tensor, which may be linearly related to displacement. The six seismic moment tensor components M_{rr} , M_{tt} , M_{pp} , M_{rt} , M_{rp} and M_{tp} , where r , t and p refer to the vertical (up), north and east directions, respectively (Aki and Richards 2002), describe the displacement field from a seismic source caused by force couples acting on particular planes. Among the six components of the centroid moment tensor, M_{rr} expresses the radial movement. Positive and negative M_{rr} represent upward and downward slip during an earthquake. Several previous studies demonstrated that

J.-Y. Lin (✉) · C.-L. Lo · J.-C. Sibuet · S.-K. Hsu
Department of Earth Sciences, National Central University,
300 Jhongda Road, Jhongli City 32001, Taoyuan County,
Taiwan, ROC
e-mail: jylin.gep@gmail.com

W.-N. Wu
Institute of Earth Sciences, Academia Sinica, 128, Sec. 2,
Academia Road, Nankang, Taipei, Taiwan, ROC

Y.-Y. Wen
Department of Earth and Environment Sciences, National Chung
Cheng University, No. 168, University Rd., Ming-Hsiung,
Chia-Yi 621, Taiwan, ROC

the M_{rr} component could be positively correlated with the state of stress (e.g., Okamoto and Tanimoto 2002). More specifically, positive and negative M_{rr} contribute to crustal thickening and extensional effects, respectively (Shapiro et al. 2004). Hence, in a complex tectonic area, the use of M_{rr} appears to be an accessible method that allows for simplification of the focal mechanism with various fault orientations and retrieval of the main deformation pattern in the vertical direction.

In the present study, we exploit the sign of one component, M_{rr} , using the global centroid moment tensor (GCMT) catalog (<http://www.globalcmt.org/>) (Dziewonski and Woodhouse 1983) to investigate the stress environment around the Sumatra area. We especially focus on the effect of the 2004 Great Sumatra–Andaman earthquake. The accumulated M_{rr} (ΔM_{rr}) was estimated, and discernibly different ΔM_{rr} distributions were observed during the inter- and post-seismic periods. The transform of M_{rr} patterns prior to and following the 2004 earthquake suggests that the intraplate stress state was changed by the earthquake.

Geological setting

In the Sumatra region, the Indian and Australian oceanic plates are subducting beneath the Sunda Plate. Because of the northward motion of the Indian and Australian oceanic plates, plate convergence becomes increasingly oblique from east to west along the Sunda and Andaman Trench (Bock et al. 2003; Michel et al. 2001) (Fig. 1a). The motion is partitioned into a component of motion normal to the trench (Bock et al. 2003; Fitch 1972; Newcomb and McCann 1987) and a right-lateral strike-slip motion along the Sumatra Fault (SF) system (Sieh and Natawidjaja 2000).

The large-scale features observed in the oceanic plate of the Wharton Basin are the Ninety East Ridge and the Investigator Fracture Zone (FZ) (98°E). Between them is a set of roughly N–S sub-parallel fracture zones identified from bathymetric, gravity and magnetic data (Liu et al. 1983; Sandwell and Smith 1994; Sibuet et al. 2007). During the inter- and post-seismic periods, a few moderate-magnitude earthquakes with N–S left-lateral and right-lateral strike-slip mechanisms occurred in both the lower plate and in the accretionary wedge (Engdahl et al. 2007; Lin et al. 2009) (Fig. 1b, c). These types of earthquakes, consistent with shear faulting on nearly N–S focal planes, were also recorded to a depth of 150 km by a local network deployed along the northern prolongation of the Investigator FZ (McCaffrey et al. 1996). Lin et al. (2009) considered that the reactivated oceanic fracture zones and the overlying sediments of the wedge functioned as a barrier

for the co-seismic rupture of the 2004 Sumatra–Andaman earthquake, underscoring the influence of the underlying active fracture zones on the structure of the upper plate. The interaction between the subduction system and the oceanic topographic feature is discussed in more detail by Dean et al. (2010) and McNeill and Henstock (2014), based on the seismic reflection and bathymetry data. They concluded that the contrasting input sediment densities on either side of the oceanic basement high at Simeulue Island appeared to affect the development of the prism and basal décollement (Dean et al. 2010). Other studies have proposed that the small scale of the fracture zones is unlikely to act as a topographic barrier to large-scale rupture during an event such as the 2004 Mw 9.3 earthquake (Tang et al. 2013). The segmentation of subduction zone rupture is more likely to be controlled by more complex origination factors. Instead of oceanic fracture zones, a thickened crustal zone in the subducting plate with compositional and topographic variations is suggested as a primary control on the upper plate structure and on the segmentation of the 2004 and 2005 earthquake ruptures. However, no matter the case, the subduction process seems largely to interact with the oceanic plate structures.

Data and analysis

Earthquake focal mechanism catalog

We evaluated the M_{rr} of the earthquakes from 1976 to 2011 using the GCMT catalog. The epicenter distribution of the mainshock and aftershocks of the Sumatra and Nias earthquake sequences are shown in Fig. 1. The magnitudes (M_w) of earthquakes were as low as 4.77, and the hypocenter depths of the aftershocks were generally shallower than 100 km (Fig. 1). The M_{rr} values from the catalog are presented as a function of temporal variation in Fig. 2a. The M_{rr} accumulation reveals that seismic moment increase was the predominant change (Fig. 2b). The two most significant positive M_{rr} values were generated by the 2004 Sumatra–Andaman and 2005 Nias earthquakes (Fig. 2a), with values of 1.04×10^{22} and 2.66×10^{21} N-m, respectively.

Spatial distribution of accumulated ΔM_{rr}

To examine the spatial distribution of ΔM_{rr} due to the 2004 Sumatra–Andaman earthquake, we divided the study area into a grid of 0.2-degree cells. M_{rr} values from all earthquakes in each individual grid cell were summed (ΔM_{rr}). To track the evolution of ΔM_{rr} , we plotted ΔM_{rr} as a function of time (Fig. 3). ΔM_{rr} estimated from seismicity prior to the 2004 Sumatra–Andaman earthquake (between

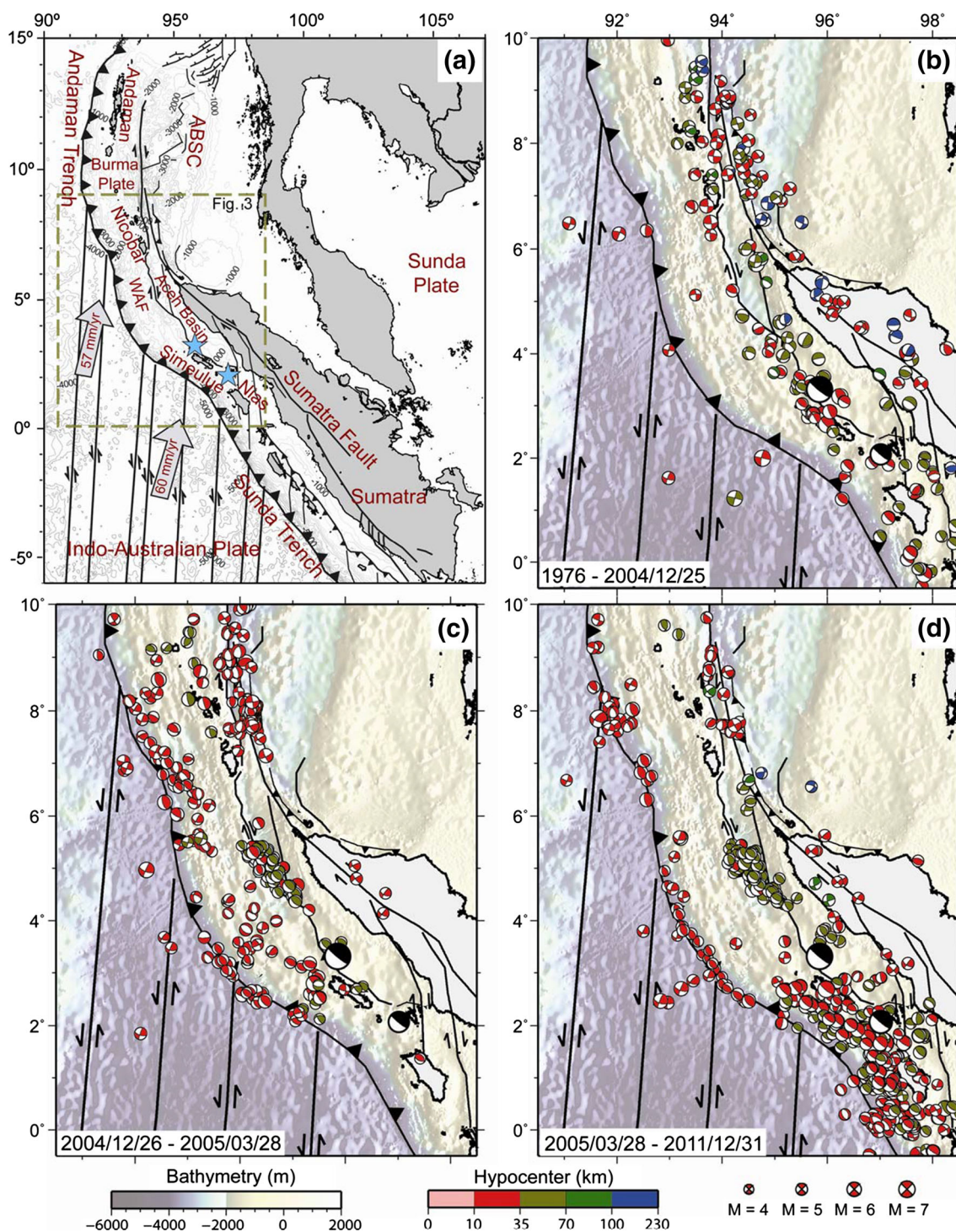
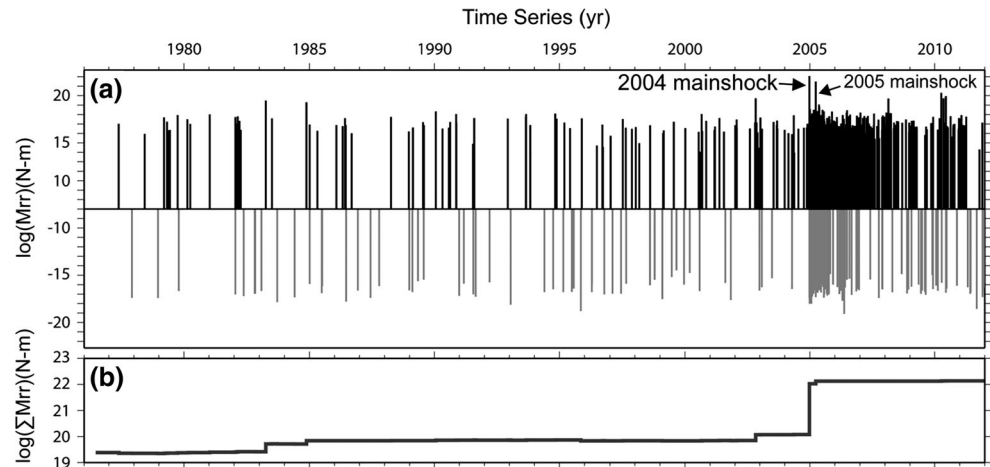


Fig. 1 a Simplified tectonic framework of the Sumatra–Andaman subduction system. *Gray arrows* indicate the NUVEL-1A relative motion between the Indo-Australian and Sunda plates (DeMets et al. 1994). The *black lines* are the main tectonic features (Pubellier et al. 2005). The Sumatra Fault is taken from Sieh and Natawidjaja (2000), the West Andaman Fault is from Martin et al. (2014), and the bathymetry and topography are from Sandwell and Smith (1994). *Light blue stars* indicate the epicenters of the 2004 Great Sumatra and 2005 Nias earthquakes. ABSC Andaman back-arc spreading center,

WAF West Andaman Fault. **b–d** Focal mechanisms from the Global CMT catalog in the Sumatra–Andaman subduction zone, with depth indicated by *color*. **b** 1976 to the Great Sumatra earthquake of 26 December 2004; **c** the 2004 mainshock to the Nias Island earthquake of 28 March 2005; **d** the 2005 Nias Island earthquake to December 2011. *Black beach balls* indicate the 2004 Mw 9.3 Great Sumatra earthquake in the north and the 2005 Mw 8.6 Nias Island earthquake in the south

Fig. 2 Temporal evolution of the radial component (Mrr) of the seismic moment solutions (a) and the Mrr accumulation (Δ Mrr) (b). Black and gray bars represent positive and negative Mrr values



1976 and the 2004 event) is shown for two depth ranges during the same time period (Fig. 3a, b).

Before the 2004 Sumatra earthquake

Before the 2004 mainshock, high Δ Mrr appears to have been concentrated along the plate interface, contributed mainly by thrusting events. A conspicuous positive Δ Mrr area parallel to the trench occurred around the location of the 2004 mainshock at a depth of approximately 30 km ($\sim 94^{\circ}$ – 96° E; 2.5° – 4.5° N) (zone A in Fig. 3a). This positive pattern corresponds to the southern end of the co-seismic vertical slip contour where the maximum co-seismic slip occurred (Ammon et al. 2005; Banerjee et al. 2007; Chlieh et al. 2007; Gahalaut et al. 2006). In contrast, a NW–SE trending zone of negative Δ Mrr was observed in the down-dip portion of the highest co-seismic slip area ($\sim 94^{\circ}$ – 96° E; 2.5° – 4.5° N), sub-parallel to the positive Δ Mrr zone mentioned previously, at a depth of 40–100 km (zone B in Fig. 3b). In addition to the earthquakes that occurred along the plate interface, the right-lateral strike-slip SF and the left-lateral strike-slip oceanic fracture zone ridges, located in the intraplate portions of the subduction system, exhibited a pattern of positive Δ Mrr at depths ranging from 0 to 40 km (zones C and D in Fig. 3a).

Several negative Mrr events were observed within the seaward side of the trench (Fig. 3a). This distribution arises from the outer-rise bending effect resulting from large compressional force applied to the subduction system. Most of this negative Δ Mrr distribution occurred next to the trench, and we do not consider these as intraplate seismic events.

For the area north of 6° N, similar to the southern part of the subduction zone, almost no earthquakes occurred in the fore-arc basin. However, farther east, a mix of positive and negative Mrr events was observed near the West Andaman Fault (WAF) (zone E in Fig. 3a).

After the 2004 Sumatra earthquake

After the 2004 mainshock, the areas with the highest Δ Mrr migrated northward beneath the Aceh Basin ($\sim 94^{\circ}$ – 95.5° E; 4° – 6° N) and westward near the trench axis ($\sim 92^{\circ}$ – 93° E; 6° – 8° N and 93° – 94° E; 2.5° – 3.5° N) (Fig. 3c, d). These Δ Mrr pattern migrations may be associated with the occurrence of plate interface afterslip events (Engdahl et al. 2007) and/or intraplate stress changes due to the highly oblique convergence of the subducting plate (Dewey et al. 2007). Otherwise, in the intraplate area, negative Δ Mrr characterized the right-lateral strike-slip SF and the left-lateral strike-slip oceanic fracture zone ridge, which is in opposition to the Δ Mrr pattern observed prior to the 2004 mainshock (zones C and D in Fig. 3c, d).

For the area north of 6° N, earthquakes that occurred in the fore-arc area show both positive and negative Mrr values. However, in the area near the WAF, in contrast to the mixed pattern of positive and negative Δ Mrr prior to the 2004 mainshock, only negative Δ Mrr was observed (zone E in Fig. 3d).

Before and after the 2005 Nias earthquake

After the 2004 Sumatra earthquake and before the 2005 Nias earthquake, only three earthquakes characterized by positive Mrr occurred south of the 2004 earthquake rupture area, in the vicinity of Simeulue and Nias Island (Fig. 3c, d). Thus, no Δ Mrr pattern was evident. After the 2005 Nias earthquake, positive Δ Mrr was observed for the fore-arc area located seaward of Simeulue and Nias Island (Fig. 3e, h). Meanwhile, several negative Mrr earthquakes occurred around Simeulue Island (Zone F in Fig. 3e). After some time, several negative Δ Mrr values were scattered about the area between the SF and the Simeulue and Nias Island (Fig. 3g).

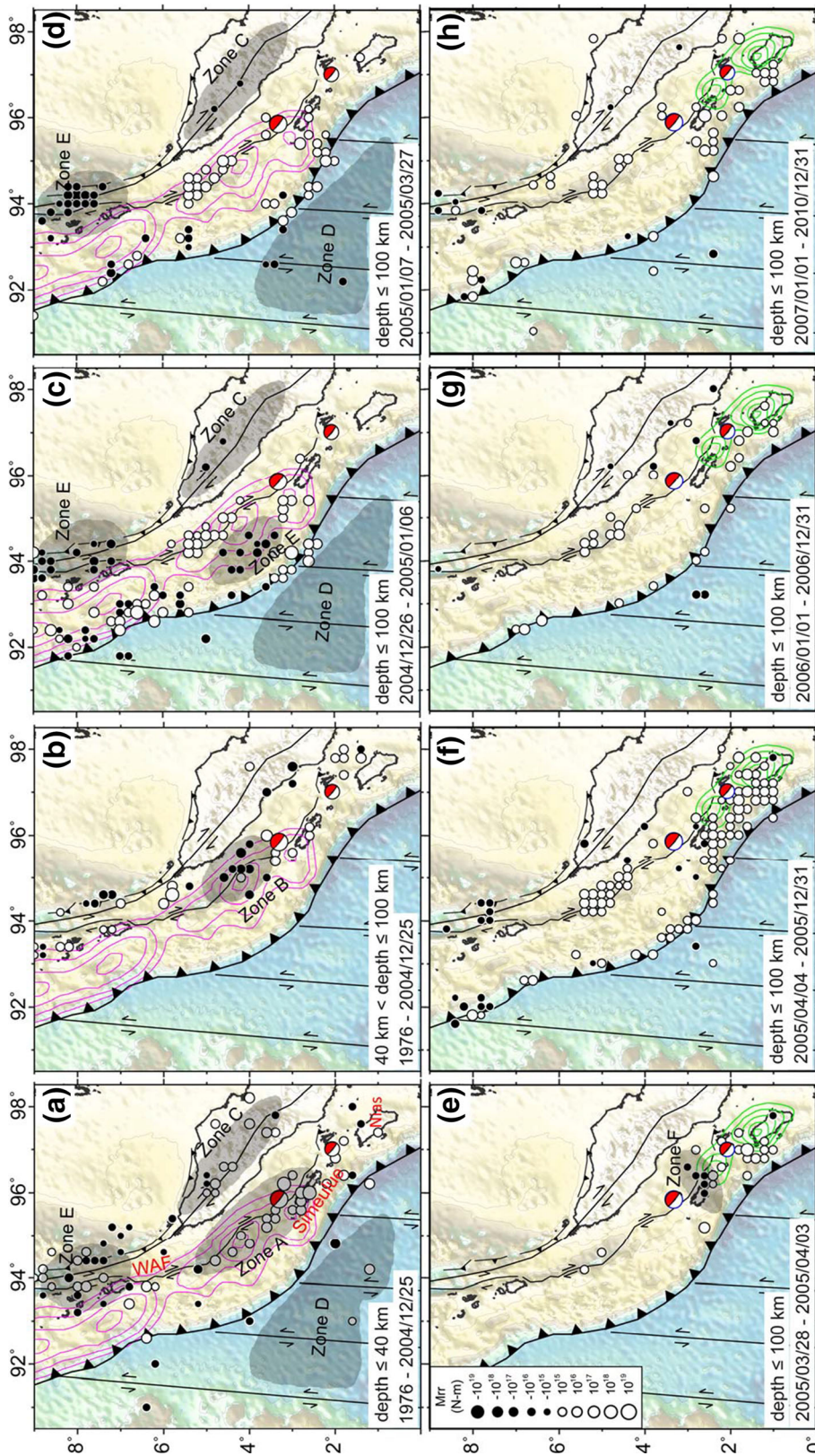


Fig. 3 Distribution of the spatial ΔM_{rr} in the Sumatra-Andaman region from 1976 to 2010. Compressional tectonic regions display a positive ΔM_{rr} (white circles), while extensional tectonic regions display a negative ΔM_{rr} (black circles). The co-seismic slip contours of the 2004 Sumatra earthquake and the 2005 Nias earthquake are shown by pink and green lines, respectively (Chlieh et al. 2007; Briggs et al. 2006). The tectonic features are as described in Fig. 1. Red beach balls represent the 2004 Sumatra-Andaman and 2005 Nias Island earthquakes

Discussion

Interplate ΔM_{rr} distribution

Compressional stress accumulation around the source area

Before the 2004 mainshock, we observed positive and negative ΔM_{rr} in zone A and B, respectively. The absence of seismicity trenchward of zone A suggests that the high positive ΔM_{rr} feature could be the down-dip limit of the inter-seismic locking zone. Some studies along the Sunda Trench have shown that the locked portion of the seismogenic zone extends from a depth of 35–57 km (Bock et al. 2003; Simoes et al. 2004; Subarya et al. 2006). Based on the high ΔM_{rr} distribution, our results suggest that the slab was locked before the mainshock with a down-dip limit at a depth of 30–40 km. At depths shallower than the down-dip limit, the plate interface was locked and few earthquakes could be observed. However, the greatest positive ΔM_{rr} in the pre-seismic period occurred in the vicinity of the down-dip limit where the 2004 mainshock was located (Figs. 1b, 3a). The presence of the pre-seismic positive ΔM_{rr} around the 2004 source area may indicate that certain amount of energy had been released in the down-dip limit of the locked zone. However, the energy released by these pre-seismic events might have not been sufficient to break through the seismic asperity until the 2004 mainshock.

Down-dip extension enhanced by the slab locking effect

A NW–SE trending negative ΔM_{rr} pattern was observed sub-parallel to the positive ΔM_{rr} zone, at a depth of 40–100 km (Zone B in Fig. 3b). The presence of this negative ΔM_{rr} reveals that the locked asperity in the shallow part of the slab may have prevented the down-dip motion of the slab. Thus, the extensional stress observed along the deeper part of the slab must be induced by the slab pull effect. The spatial distribution of this negative ΔM_{rr} feature is limited to the area between 3.5°N and 5.0°N, approximately 180 km in length. The co-seismic rupture of the 2004 great Sumatra earthquake propagated approximately 1,300 km northward from the mainshock (Ishii et al. 2007). Thus, the length dimension of the down-dip extension portion is less than one-sixth that of the co-seismic rupture area. This means that, although the 2004 event ruptured the entire 1,300 km area, the main locking effect should be located in the most southern portion of the co-seismic slip zone, around the source area, and should reinforce the effect of slab pull. However, from another point of view, the extremely oblique subduction along the north Sunda subduction system may cause a small component of slab motion along a direction perpendicular to the subduction system. Consequently, the relatively small

trench-normal component along the northern part of the subduction system may reduce the subduction portion of the slab and decrease the slab pull effect. This may be the reason why we could not observe an obvious slab pull effect around the area.

In contrast to the 2004 earthquake, few earthquakes occurred in the rupture area of the 2005 event prior to its occurrence. Because the timing of the 2004 and 2005 events was very close, the pre-seismic characteristics of the 2005 earthquake may have been influenced by the 2004 event. Thus, no clear pre-seismic M_{rr} pattern was evident for the 2005 earthquake.

Crustal resilience effect

Figure 3c shows the ΔM_{rr} distribution during the 10 days following the 2004 mainshock. Most events that occurred at or immediately east of the trench following the 2004 mainshock were thrust or strike-slip faulting mechanisms (Fig. 1c). However, in the northwestern part of the 2004 mainshock, approximately 100–150 km from the trench axis, a series of negative M_{rr} events, trending sub-parallel to the trench, struck the fore-arc area ($\sim 93^\circ$ – 95° E; 3.0° – 5.0° N) (zone E in Fig. 3c). Surprisingly, this pattern of negative ΔM_{rr} completely disappeared 10 days after the mainshock (Fig. 3c, d). A similar pattern was also observed after the 2005 Nias earthquake. Several events characterized by negative M_{rr} occurred in the north of Simeulue Island during a short period of 5 days. Although some negative M_{rr} values subsequently appeared in the area, the frequency of their occurrence was much lower (approximately one negative M_{rr} earthquake every 2–3 months).

The negative ΔM_{rr} patterns observed at depths of 20–30 km may have been related to the subsidence caused by the post-seismic crustal resilience on the down-dip end of the rupture, a scenario akin to the elastic slip dislocation model described by Meltzner et al. (2006). These earthquakes were caused by the elastic slip dislocation of the rupture when the large subduction event occurred: the up-dip portion may have recovered the energy stored during the inter-seismic period and experienced a sudden uplift motion, while the down-dip end subsided (Meltzner et al. 2006).

According to this hypothesis, the sudden disappearance of negative ΔM_{rr} within 10- and 5-day periods indicates that the duration of the crustal resilience effect on the down-dip end of the rupture was significantly shorter than that of the aftershock activity. Generally, the post-seismic visco-elastic relaxation is sustained for several months or even years, and the affected depth often includes the mantle portion. Although the mechanism for this kind of resilience is similar to visco-elastic relaxation, the short duration and lower influenced depths of this effect indicate

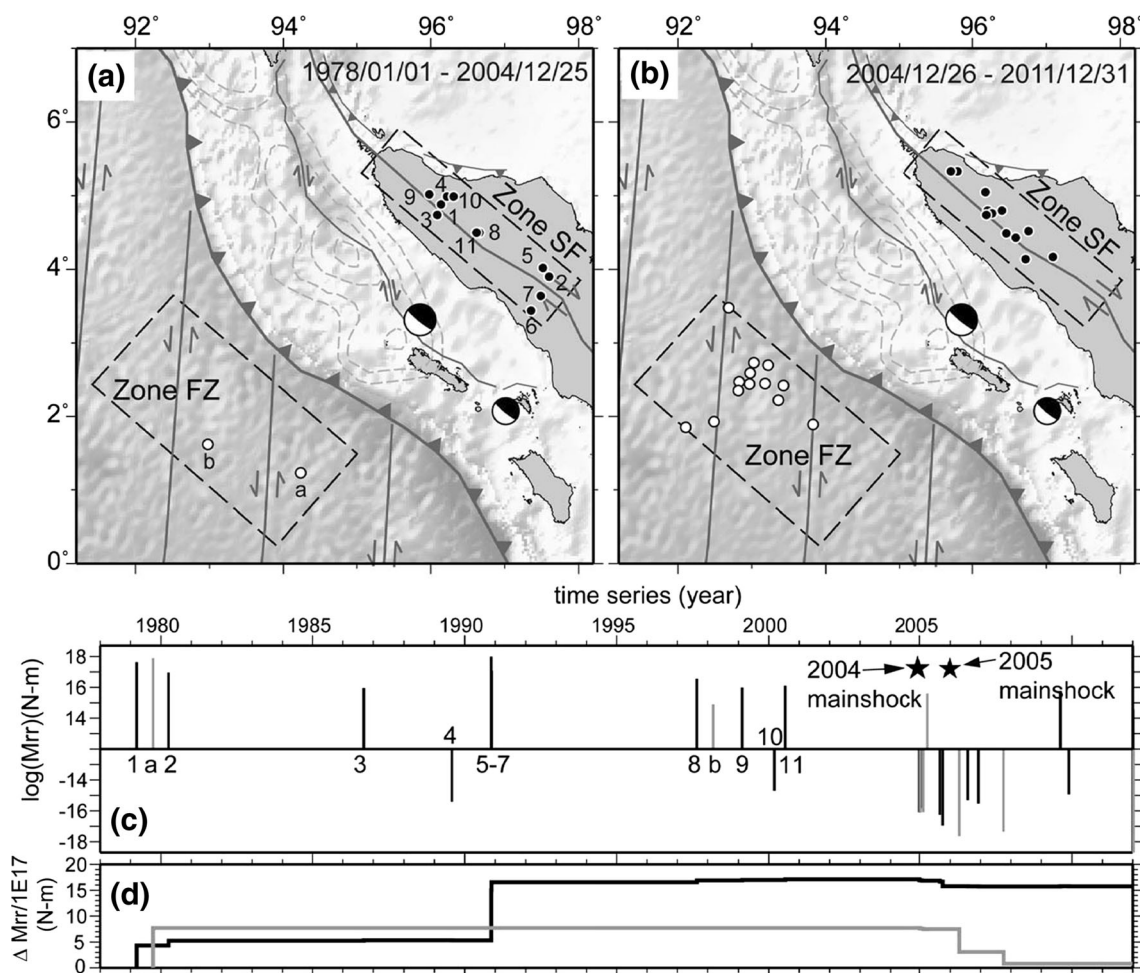


Fig. 4 Earthquakes used for the analyses of Mrr and ΔMrr in the SF and oceanic fracture zones (FZ) are shown by *white* and *black* dots in (a, b). The 5-m co-seismic slip contours in *gray dashed lines* are from Chlieh et al. (2007). c, d The Mrr and the Mrr accumulation (ΔMrr).

Light gray and *black* lines show the Mrr obtained from the FZ and SF zones, respectively. *Black stars* are the 2004 Sumatra–Andaman and 2005 Nias Island earthquakes

that a different process prevails. However, this type of event was rarely observed. Their presence could be affected by various conditions, such as the degree of interplate coupling and the distribution of rupture slip, among others. It is difficult to investigate this issue given the limited data and study area of the present work. Further investigations on other plate interface events are required to further understand the characteristics of these processes.

Intraplate pre- and post-seismic stress state variations

It is remarkable that the right-lateral strike-slip SF and the left-lateral strike-slip oceanic fracture zone ridge exhibited a pattern of positive ΔMrr prior to the 2004 mainshock (zones C and D in Fig. 3a) and a pattern of negative ΔMrr immediately after (zones C and D in Fig. 3c, d). To further analyze this evident change, we examined the Mrr value of the earthquakes located along the SF (Zone SF) and the

oceanic fracture zone (Zone FZ) areas and its temporal variation (Fig. 4).

Tectonic significance of the pre- and post-seismic ΔMrr distribution

Before the 2004 mainshock, only 11 and 2 events were located in the SF and FZ areas, respectively (numbered dots in Fig. 4a). Except for two events (No. 4 and 10), the earthquakes are characterized by positive Mrr, with a value between 10^{16} and 10^{18} N-m (Fig. 4c). The ΔMrr values calculated from earthquakes since 1978 for the SF and FZ zones are approximately 1.71×10^{18} and 7.71×10^{17} N-m (Fig. 4d), or approximately 0.016 and 0.00074 % of the Mrr produced by the 2004 Sumatra mainshock, respectively. Also, relatively more earthquakes occurred in our research areas after the 2004 main event (Fig. 4b). In contrast to what occurred before the 2004 mainshock, almost all the

aftershocks show negative M_{rr} values (Fig. 4c). From the 2004 mainshock until the end of 2011, the ΔM_{rr} has dropped by 1.3×10^{17} and 6.93×10^{17} N-m for the SF and FZ zones.

The results mentioned previously show that intraplate stress has affected the continental and oceanic areas and has caused positive and negative ΔM_{rr} distributions for the pre- and post-mainshock period. These changes may be attributed to a stress release mechanism associated with an intraplate stress decrease after the mainshock, which was induced by the unlocking of the asperities. Prior to the mainshock, the stress accumulated in the locked zone might squeeze both the subducting and overriding plates and compress the SF and the oceanic fracture zones. Thus, almost all the intraplate earthquakes that occurred before the mainshock were characterized by positive M_{rr} . However, the occurrence of the 2004 mainshock may have removed the stress source and resulted in an extensional environment along the SF and the oceanic fracture zones immediately after the mainshock. This mechanism was well illustrated by the dominant distribution of the negative ΔM_{rr} in the intraplate area.

Other evidence for intraplate stress changes

As mentioned previously, few earthquakes occurred in the rupture zone of the 2005 earthquake prior to its mainshock. Similarly, almost no earthquake occurred along the oceanic fracture zone and the SF near the portion of the 2005 rupture zone. Thus, no clear pre-seismic effect can be observed. However, the sparse negative M_{rr} earthquakes spreading between the SF and Simeulue and Nias Islands after the 2005 event illustrated same post-seismic characteristics as the 2004 earthquake (Fig. 3g).

The WAF area connects the SF in the south and the Andaman Spreading Center in the north. The complex geological environment in the area is evidenced by the mixed distribution of positive and negative M_{rr} events before the 2004 mainshock (Zone E in Fig. 3a). However, after the mainshock, only earthquakes with negative M_{rr} occurred (Zone E in Fig. 3d–h). This observation may also infer a stress decrease in the overriding plate.

Most destructive earthquakes occur along subduction zones. The stress state along subduction systems has been always an important issue for seismic hazard assessment. However, most subduction zones are located in marine areas, where the acquisition of data for stress analyses is generally difficult. Our study shows that the influence of a locked subduction portion could be observed in the intraplate area of both the overriding and the subducting plates. This result provides an accessible approach for research of subduction zones. Finally, it is

worth pointing out that the positive and negative M_{rr} observed along the SF and the oceanic fracture zone was predominantly obtained from strike-slip events rather than thrusting or normal earthquakes. The strike-slip events often contain a compressive or extensional component, which is generally minor and difficult to observe by inspection of focal mechanisms. However, our results demonstrate that the use of M_{rr} is a valid approach to understand further tectonic stress constraints in subduction systems.

Conclusions

Complex tectonic environments, such as subduction systems, are generally illustrated by focal mechanisms with various fault orientations. The strike-slip events often contain a compressive or extensional component, which is generally minor and difficult to observe by inspection of focal mechanisms. Therefore, the analysis of M_{rr} variation provides an accessible method to more easily understand the main stress regime without being distracted by various fault configurations. In our study, we examined the changes in ΔM_{rr} distribution in the Sumatra area from January 1976 to December 2010. Prior to the 2004 Sumatra–Andaman earthquake mainshock, the highest ΔM_{rr} was located near the source area ($\sim 95.5^\circ\text{E}$; 3°N), indicating that a large amount of stress was accumulating in its vicinity. On the landward side of this feature, a trench-parallel negative ΔM_{rr} pattern spreading along the slab at a depth of 40–100 km was observed, which was indicative of a down-dip extension mechanism (Fig. 3b). The presence of a locked seismogenic zone in the shallow part may prevent the down-dip motion of the slab, enhance the slab pull force and create a relatively extensional mechanism. Pre-seismic positive ΔM_{rr} was observed along the right-lateral strike-slip SF and the oceanic fracture zones (Fig. 3a), revealing the existence of intraplate compression mechanisms in both the upper and lower plates. After the mainshock, however, the two areas were characterized by negative ΔM_{rr} , indicating a release of stress associated with a decrease of intraplate stress caused by the unlocking of the asperities.

Acknowledgments We thank the editor, Dr. Chun-Feng Li, and one anonymous reviewer for their helpful comments. Special thanks are given to Dr. Sean Gulick, one of the reviewers, for his pertinent and valuable remarks and suggestions. Figures were prepared with the Generic Mapping Tool (GMT) software (Wessel and Smith 1998). This research was supported by the Taiwan Earthquake Research Center (TEC) and funded through Ministry of Science and Technology (MOST) with grant numbers MOST-103-3113-M-008-001 and MOST-103-2116-M-008-017.

References

- Aki K, Richards PG (2002) *Quantitative seismology*. University Science Books, Sausalito
- Ammon CJ, Ji C, Thio HK, Robinson D, Ni SD, Hjorleifsdottir V, Kanamori H, Lay T, Das S, Helmlinger D, Ichinose G, Polet J, Wald D (2005) Rupture process of the 2004 Sumatra–Andaman earthquake. *Science* 308(5725):1133–1139
- Banerjee P, Pollitz F, Nagarajan B, Bürgmann R (2007) Coseismic slip distributions of the 26 December 2004 Sumatra–Andaman and 28 March 2005 Nias earthquakes from GPS static offsets. *Bull Seismol Soc Am* 97(1A):S86–S102
- Bilham R, Engdahl R, Feldl N, Satyabala S (2005) Partial and complete rupture of the Indo–Andaman plate boundary 1847–2004. *Seismol Res Lett* 76(3):299–311
- Bock Y, Prawirodirdjo L, Genrich JF, Stevens CW, McCaffrey R, Subarya C, Puntodewo SSO, Calais E (2003) Crustal motion in Indonesia from global positioning system measurements. *J Geophys Res*. doi:10.1029/2002GL015215
- Briggs RW, Sieh K, Meltzner AJ, Natawidjaja D, Galetzka J, Suwargadi B, Hsu Y-J, Simons M, Hananto N, Suprihanto I (2006) Deformation and slip along the Sunda megathrust in the great 2005 Nias–Simeulue earthquake. *Science* 311(5769):1897–1901
- Chlieh M, Avouac JP, Hjorleifsdottir V, Song TRA, Ji C, Sieh K, Sladen A, Hebert H, Prawirodirdjo L, Bock Y, Galetzka J (2007) Coseismic slip and afterslip of the great M-w 9.15 Sumatra–Andaman earthquake of 2004. *Bull Seismol Soc Am* 97(1):S152–S173
- Dean SM, McNeill LC, Henstock TJ, Bull JM, Gulick SP, Austin JA, Bangs NL, Djajadihardja YS, Permana H (2010) Contrasting décollement and prism properties over the Sumatra 2004–2005 earthquake rupture boundary. *Science* 329(5988):207–210
- DeMets C, Gordon RG, Argus DF, Stein S (1994) Effect of recent revisions to the geomagnetic reversal time scale on estimates of current plate motions. *Geophys Res Lett* 21(20):2191–2194
- Dewey JW, Choy G, Presgrave B, Sipkin S, Tarr AC, Benz H, Earle P, Wald D (2007) Seismicity associated with the Sumatra–Andaman Islands earthquake of 26 December 2004. *Bull Seismol Soc Am* 97(1):S25–S42
- Dziewonski AM, Woodhouse JH (1983) An experiment in systematic study of global seismicity: centroid-moment tensor solutions for 201 moderate and large earthquakes of 1981. *J Geophys Res* 88(B4):3247–3271
- Engdahl ER, Villasenor A, DeShon HR, Thurber CH (2007) Teleseismic relocation and assessment of seismicity (1918–2005) in the region of the 2004 M-w 9.0 Sumatra–Andaman and 2005 M-w 8.6 Nias Island great earthquakes. *Bull Seismol Soc Am* 97(1):S43–S61
- Fitch T (1972) Plate convergence, transcurrent faults, and internal deformation adjacent to Southeast Asia and the Western Pacific. *J Geophys Res* 77(23):4432–4460
- Gahalaut V, Nagarajan B, Catherine J, Kumar S (2006) Constraints on 2004 Sumatra–Andaman earthquake rupture from GPS measurements in Andaman–Nicobar Islands. *Earth Planet Sci Lett* 242(3):365–374
- Ishii M, Shearer PM, Houston H, Vidale JE (2007) Teleseismic P wave imaging of the 26 December 2004 Sumatra–Andaman and 28 March 2005 Sumatra earthquake ruptures using the Hi-net array. *J Geophys Res*. doi:10.1029/2006JB004700
- Lin J-Y, Le Pichon X, Rangin C, Sibuet J-C, Maury T (2009) Spatial aftershock distribution of the 26 December 2004 great Sumatra–Andaman earthquake in the northern Sumatra area. *Geochem Geophys Geosyst*. doi:10.1029/2009GC002454
- Liu C, Curry JR, McDonald JM (1983) New constraints on the tectonic evolution of the eastern Indian Ocean. *Earth Planet Sci Lett* 65(2):331–342
- Martin KM, Gulick SP, Austin JA, Berglar K, Franke D (2014) The West Andaman Fault: a complex strain-partitioning boundary at the seaward edge of the Aceh Basin, offshore Sumatra. *Tectonics*. doi:10.1002/2013TC003475
- McCaffrey R, Wark D, Sunaryo, Prih Haryadi PY (1996) Lateral variation in slab orientation beneath Toba caldera, northern Sumatra. *Geophys Res Lett* 23(5):443–446
- McNeill LC, Henstock TJ (2014) Forearc structure and morphology along the Sumatra–Andaman subduction zone. *Tectonics* 33(2):112–134
- Meltzner AJ, Sieh K, Abrams M, Agnew DC, Hudnut KW, Avouac JP, Natawidjaja DH (2006) Uplift and subsidence associated with the great Aceh–Andaman earthquake of 2004. *J Geophys Res*. doi:10.1029/2005JB003891
- Michel GW, Yu YQ, Zhu SY, Reigber C, Becker M, Reinhart E, Simons W, Ambrosius B, Vigny C, Chamot-Rooke N, Le Pichon X, Morgan P, Matheussen S (2001) Crustal motion and block behaviour in SE-Asia from GPS measurements. *Earth Planet Sci Lett* 187(3):239–244
- Newcomb KR, McCann WR (1987) Seismic history and seismotectonics of the Sunda Arc. *J Geophys Res* 92(B1):421–439
- Okamoto T, Tanimoto T (2002) Crustal gravitational energy change caused by earthquakes in the western United States and Japan. *Earth Planet Sci Lett* 195(1–2):17–27
- Pollitz FF, Bürgmann R, Banerjee P (2006) Post-seismic relaxation following the great 2004 Sumatra–Andaman earthquake on a compressible self-gravitating Earth. *Geophys J Int* 167(1):397–420
- Pubellier M, Rangin C, Le Pichon X, Ego F, Nielsen C, Rabaut A, Ngoc Nguyen HT, Pagot P, Tsang Hin Sun D (2005) DOTSEA—a synthesis of deep marine data in Southeast Asia. *Soc Geol Fr* 176:1–32
- Reddy C, Prajapati SK, Sunil P (2010) Co and postseismic characteristics of Indian sub-continent in response to the 2004 Sumatra earthquake. *J Asian Earth Sci* 39(6):620–626
- Sandwell DT, Smith WHF (1994) New global marine gravity map/grid based on stacked ERS1, Geosat and Topex altimetry. *Eos Trans AGU* 75(16)(Spring Meet. Suppl.):321
- Shapiro NM, Ritzwoller MH, Molnar P, Levin V (2004) Thinning and flow of Tibetan crust constrained by seismic anisotropy. *Science* 305(5681):233–236
- Sibuet J-C, Rangin C, Le Pichon X, Singh S, Cattaneo A, Graindorge D, Klingelhoefer F, Lin J-Y, Malod J, Maury T, Schneider J-L, Sultan N, Umber M, Yamaguchi H, “Sumatra aftershocks” Team (2007) 26th December 2004 great Sumatra–Andaman earthquake: co-seismic and post-seismic motions in northern Sumatra. *Earth Planet Sci Lett* 263(1):88–103
- Sieh K, Natawidjaja D (2000) Neotectonics of the Sumatra fault, Indonesia. *J Geophys Res* 105(B12):28295–28326
- Simoes M, Avouac JP, Cattin R, Henry P (2004) The Sumatra subduction zone: a case for a locked fault zone extending into the mantle. *J Geophys Res*. doi:10.1029/2003JB002958
- Subarya C, Chlieh M, Prawirodirdjo L, Avouac JP, Bock Y, Sieh K, Meltzner AJ, Natawidjaja DH, McCaffrey R (2006) Plate-boundary deformation associated with the great Sumatra–Andaman earthquake. *Nature* 440(7080):46–51
- Tang G, Barton PJ, McNeill LC, Henstock TJ, Tilmann F, Dean SM, Jusuf MD, Djajadihardja YS, Permana H, Klingelhoefer F (2013) 3-D active source tomography around Simeulue Island offshore Sumatra: thick crustal zone responsible for earthquake segment boundary. *Geophys Res Lett* 40(1):48–53
- Verma R, Mukhopadhyay M, Bhuin N (1978) Seismicity, gravity, and tectonics in the Andaman sea. *J Phys Earth* 26(Suppl):S233–S248
- Wessel P, Smith WHF (1998) New, improved version of Generic Mapping Tools released. *Eos Trans AGU* 79(47):579
- Zhou Y, Xu L, Chen Y (2002) Source process of the 4 June 2000 southern Sumatra, Indonesia, earthquake. *Bull Seismol Soc Am* 92(5):2027–2035